Materials Science in Semiconductor Processing 80 (2018) 52–55

Contents lists available at ScienceDirect

Materials Science in Semiconductor Processing

journal homepage: www.elsevier.com/locate/mssp

Photoluminescence study of deep donor- deep acceptor pairs in Cu_2ZnSnS_4

J. Krustok[a,b,*], T. Raadik[b], M. Grossberg[b], M. Kauk-Kuusik[b], V. Trifiletti[c], S. Binetti[c]

[a] Division of Physics, Tallinn University of Technology, Ehitajate Tee 5, 19086 Tallinn, Estonia
[b] Department of Materials and Environmental Technology, Tallinn University of Technology, Ehitajate Tee 5, 19086 Tallinn, Estonia
[c] Department of Materials Science and Solar Energy Research Center (MIB-SOLAR), University of Milano-Bicocca, Via Cozzi 55, I-20125 Milano, Italy

ARTICLE INFO

Keywords:
Cu_2ZnSnS_4
Photoluminescence
Donor-acceptor pairs
Defects
Kesterites

ABSTRACT

We present photoluminescence (PL) studies of high quality Cu_2ZnSnS_4 single crystals and thin films. At T = 10 K two PL bands (D_1 and D_2) were detected in both samples at about 1.35 eV and 1.27 eV. The temperature and laser power dependencies indicate that the properties of PL bands can be explained by deep donor-deep acceptor pair model, where the D_1 and D_2 bands result from a recombination between pairs of the closest neighbors, and between pairs of the next-closest neighbors, respectively. The donor defect in these pairs is suggested to be an interstitial Zn atom and located in either of the two possible interstitial positions. The most probable deep acceptor defect in this pair is Cu_{Zn}.

1. Introduction

The kesterites Cu_2ZnSnS_4 (CZTS) and $Cu_2ZnSnSe_4$ (CZTSe) are attracting extensive interest as cheaper absorber materials for solar cells because first principles calculations predict that their electronic properties must be similar to more expensive chalcopyrite $Cu(In,Ga)Se_2$ (CIGSe) compounds, which already have shown quite high solar cell efficiency exceeding 22% [1]. However, the highest solar cell efficiency published for kesterites is only 12.6% [2]. To further improve the conversion efficiency of indium free kesterite solar cells, it is important to get more detailed information about different defects in CZTS-based materials. Photoluminescence (PL) spectroscopy is a powerful optical method for the characterization of defects in many semiconductor materials. Unfortunately, even the low temperature ($T \sim 10$ K) PL emission in CZTS usually shows a wide and single asymmetrical PL band at around 1.3 eV often affected by conduction and valence band tails [3–8]. These tails are created due to high concentration of different charged defects and the main recombination path often goes through these tails giving very little information about particular defects. At the same time, the PL band at 1.3 eV has shown somewhat different properties in different CZTS samples. In Ref [4], for example, it was found that the PL emission at 1.3 eV in slightly Cu-rich CZTS polycrystals consists of two PL bands at 1.27 eV and 1.35 eV that both result from band-to-deep acceptor (E_a = 280 meV) recombination in disordered and ordered CZTS, respectively. On the other hand, for the same PL band in CZTS, very different thermal quenching activation energies 48 meV [9], 39 meV and 59 meV [10], 29–40 meV [11] and 140 meV [12] have been also reported. Rather low activation energies and rather deep PL band ($E_g \sim 1.64$ eV at T = 10 K [13]) suggest that in many cases defect complexes are involved in the recombination process. Theoretical calculations have also shown that the formation of various defect complexes is highly probable in CZTS [14–18]. In our previous study [6], we showed that the recombination between electrons and holes in a quantum well, caused by the defect clusters that induce a significant local band gap decrease of 0.35 eV in CZTS, is characterized by a relatively low ($E_a < 100$ meV) thermal quenching activation energy. Also the quasi donor-acceptor pair (QDAP) model is often proposed to support the 1.3 eV PL band in CZTS [19–21]. Moreover, the peak position of this PL band depends on fraction of disordered kesterite phase in CZTS [5]. Usually in disordered structure the PL peak is red-shifted about 100 meV due to smaller band gap energy [4,22]. Therefore the presence of partial disordering can cause also spatial band gap energy fluctuations. So the varying behavior of the 1.3 eV PL band can be explained by different recombination mechanisms in samples with different chemical and structural composition although the PL emission falls into the same spectral region. One reason for this diversity is the variable quality of studied thin films or crystals. Almost all experimental studies on CZTS have shown that this absorber material has a very high concentration of charged point defects and these defects are responsible for the spatial electrostatic potential fluctuations. Relatively deep potential fluctuations and possible band gap energy fluctuations determine also the width (and shape) of PL bands and even at very low temperatures it is difficult to resolve all possible recombinations. The average depth of potential fluctuations γ (determined from the low-energy side of the PL band) in CZTS is about 50 meV [3,23,24], but γ values as low as 11 meV [4] and 22 meV [5]

* Corresponding author at: Department of Materials and Environmental Technology, Tallinn University of Technology, Ehitajate Tee 5, 19086 Tallinn, Estonia.
E-mail address: Juri.Krustok@ttu.ee (J. Krustok).

https://doi.org/10.1016/j.mssp.2018.02.025
Received 20 November 2017; Received in revised form 5 February 2018; Accepted 17 February 2018
Available online 22 February 2018
1369-8001/

were also reported. Therefore, it is obvious that for better understanding of PL processes samples with $\gamma < 25$ meV must be used.

In this report we present PL studies of high quality CZTS single crystal (SC) grown by iodine transport and CZTS thin film (TF) prepared by using sol-gel technology and show, that the PL emission at 1.3 eV in both samples involves two bands related to deep donor- deep acceptor pairs with different distance between donor and acceptor defects.

2. Experimental

The Cu_2ZnSnS_4 single crystals were grown via chemical vapor transport using iodine as a transport agent. Previously synthesized $Cu_{1.82}Zn_{1.12}SnS_{3.97}$ powder (3 N purity) was mixed together with 4 N purity CuI (5 mg of iodine per cm^3) and sealed in evacuated quartz ampoule. The sealed ampoule was placed in a two-zone horizontal furnace. Both temperature zones were heated up to 600 °C with the heating rate 2 °C/min and maintained at this temperature for 24 h. After that the temperatures at source and growth zones were raised up to 750 and 650 °C with the heating rate 2 °C/min, respectively. Crystal growth process took place at these temperature regimes for 2 weeks. After this, both zones were cooled down to room temperature (RT) with the cooling rate 3 °C/min. The chemical formula of single crystals calculated from EDX analysis data was $Cu_{1.87}Zn_{1.02}SnS_{3.87}$.

The sol-gel for CZTS thin films was prepared in a reaction flask by dissolving copper (II)-acetate monohydrate (2 N purity, 0.25 M), tin(II)-chloride dihydrate (2 N purity, 0.125 M), zinc(II)-acetate dihydrate (4 N purity, 0.125 M) and thiourea (2 N purity, 2.5 M) into dimethyl sulfoxide (3 N purity) by magnetic stirring for overnight at RT. Then the cap was removed and the solution left to rest until full gel formation. The resulting white and opaque gel was deposited onto a fluorine-doped tin oxide coated glass via doctor blade coating, using a Kapton tape mask; the resulting film was first annealed at 200 °C onto a hot-plate for 30 min (heating rate 3 °C/min) under nitrogen flow, subsequently the tape was removed and the layer sintered in oven under argon flow at 550 °C for 30 min (heating rate 2 °C/min). The sample was slowly cooled down in the furnace and stream of argon was turned off at 280 °C. The chemical formula of CZTS thin film calculated from EDX analysis data was $Cu_{2.02}Zn_{1.07}SnS_{4.02}$.

Raman spectra were recorded by using a Horiba's LabRam HR800 spectrometer and 532 nm laser line that was focused on the sample with spot size of about 5 μm. A 0.64 m focal length single grating (600 mm^{-1}) monochromator and the 442 nm line of a He-Cd laser with different power were used for the photoluminescence measurements. A closed-cycle helium cryostat was employed to measure temperature dependencies of the PL spectra at temperatures from 10 K to 300 K. The PL signal was detected by an InGaAs detector.

3. Results and discussion

Fig. 1(a) presents room temperature Raman spectra of both CZTS samples. Raman peak parameters were determined by fitting spectra with Lorentzian curves. The main A_1 peak of TF sample at 339 cm^{-1} has a halfwidth of $W = 2.7$ cm^{-1} and this quite small value verifies a good quality of CZTS. The halfwidth of the same peak in SC sample was slightly higher: $W = 3.8$ cm^{-1}. The presence of a small additional Raman peak at 335 cm^{-1} giving a shoulder to the CZTS A_1 peak at 339 cm^{-1} is observed in both samples and this peak is believed to be related to disordered kesterite phase in CZTS [4,25]. Again, the relative intensity of the 335 cm^{-1} peak was higher in SC sample. This small difference between TF and SC samples is probably related to a slightly different cooling rate after high temperature treatment of both samples. Although the slow cooling rate after the growth must result in an ordered phase [5], we are still able to detect a small fraction of disordered CZTS. The disordered kesterite phase typically involves a high concentration of antisite defects like Cu_{Zn} or Zn_{Cu} [26,27]. No other phases were detected by Raman measurements.

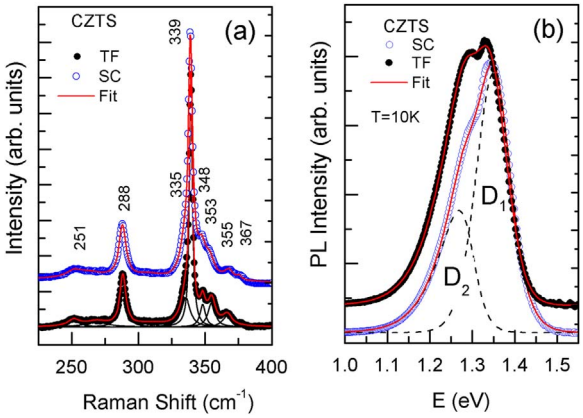

Fig. 1. (a) Room temperature Raman spectra and (b) low temperature PL spectra of CZTS single crystal (SC) and thin film (TF) samples together with fitting results (red lines). Spectra are vertically shifted for clarity.

Fig. 1(b) shows typical PL spectra of SC and TF CZTS at $T = 10$ K. Two asymmetric PL bands D_1 and D_2 are clearly visible at about 1.35 eV and 1.27 eV, respectively. All PL spectra were fitted using asymmetric double sigmoidal function [28] and the fitting result for SC sample is also shown in Fig. 1(b). The average depth of the potential fluctuations γ was determined from the exponential slope of the low-energy side of PL bands and was found to be around 25 meV for both samples. The separation between D_1 and D_2 PL bands was about 80 meV. The high-energy band (D_1) in both samples shows more rapid quenching with temperature, see Fig. 2(a). Arrhenius plots of the resulting integral intensities for both bands of SC sample are shown in Fig. 2(b). The best fits have been achieved for a single recombination channel and assuming a temperature dependence of the hole capture cross section proposed in [29]: $I(T) = I/[1 + A_1T^{3/2} + A_2T^{3/2} exp(-E_a/kT)]$, where I is the integral intensity of the PL band, A_1 and A_2 are process rate parameters and E_a is the activation energy. Obtained activation energies for D_1 and D_2 bands in SC sample were $E_a = 105$ meV and $E_a = 125$ meV, respectively. Thin film sample showed quite similar behavior with temperature. Although the double peak structure of the PL emission seems to be very similar to the structure reported in [4], the temperature dependence of this PL emission is different. Both PL bands in Ref. 4 showed very high temperature quenching activation energy $E_a \sim 280$ meV and the laser power dependence of the low-temperature PL spectrum revealed a strong blue shift of 15 meV per decade of both bands. In the present case such a strong blue shift was not observed, see Fig. 3(a). On the contrary, we observe very small red shift (≤ 2 meV per decade) for both bands and therefore it is obvious that D_1 and D_2 PL bands in our samples have different origin. Very similar D_1 and D_2

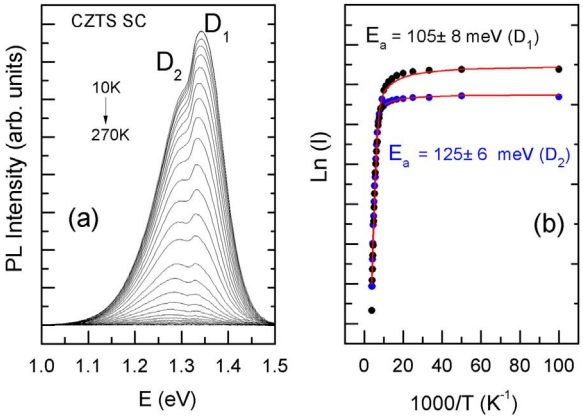

Fig. 2. (a) Temperature dependence of PL bands; (b) Arrhenius plots of integral intensity for D_1 and D_2 PL bands with fitting results of CZTS SC sample.